IAPR Workshop on CV - Special Hardware and Industrial Applications OCT.12-14, 1988, Tokyo

Automatic Inspection of Diode Pellets

Yoshikuni Okawa*, and Seiji Mizuno**

*Osaka University
Yamada-Oka, Suita, Osaka 565

**Gifu University
Yanagido,Gifu, 501-11

Abstract

We will report the results of applying the image processing techniques to the automatic inspection of diode pellets.

The inspection items are: (1) their geometrical form, and (2) stains on the bonding surface. The decision rule is based on the statistical decision theory concerning the variables measured from digitized images. Six parameters are calculated in each sample, and compared with the prespecified thresholding values, which decides the sample to be accepted or rejected.

About 97 % of the computer's decision are proved to be correct by the human experienced inspectors.

1. Introduction

It has long been pointed out that the picture processing technology can be applied to the automation of various inspection processes in factories [1],[2]. Many case studies, such as reed switches[3], printed circuit boards[4], billets[5], cast irons[6] have been reported elsewhere, which consist only a few among many other available examples. In the most advanced production processes the picture processing technology has already been realized.

Human inspectors see diode pellets through a microscope, and decide whether it is acceptable or not. The feasibility of visual inspection is based on the fact that a form of a pellet is closely related to its electrical characteristics. That is, if a pellet (PN junction) is deformed, then , for example, its nominal current capacity decreases. Therefore, by the visual inspection of pellets or rejecting deformed pellets, the quality of the product can be stabilized.

Visual inspection is a bitter and hard work to human labors where computers are successfully replaced for their hardships using the recently advanced picture processing technology.

2. Diode Pellets and Its Inspection

A shape of a diode pellet is shown in Fig. 1, which is technically a P-N junction. A lead wire is bonded to a pellet as shown in Fig. 2.

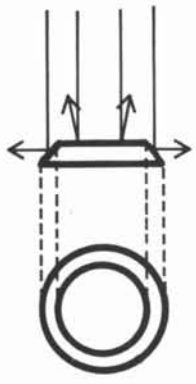

Fig.1 A pellet.

Fig.2 The lead wire.

We have two major inspection items: 1. the geometrical constitution of a pellet, and 2. the status of the upper bonding area.

If a pellet is deformed, its electrical characteristic will decline. Contamination on the bonding area causes the contact resistance high.

Three photographs are shown in Fig. 3: (a) a normal (or acceptable) pellet, (b) a deformed pellet, and (c) a stained pellet. Both (b) and (c) should be rejected by the inspection. The size of a pellet relates its electrical capacities. We use two kinds of pellets of different size: one is 2.8 mm in its diameter, and the other is 1.85 mm. A pellet is placed on the sample table of the microscope and a light source drops its coherent illuminating rays vertically.

An industrial TV camera is attached to the microscope instead of an eyepiece. The output voltage of the TV camera is digitized by an AD converter (8 bit or 256 gray levels), and these numerics are stored in the memory of a personal computer. The grid points are 320x240.

A diameter of a pellet is adjusted by the microscope, so as to have just 120 pixels in its widest horizontal diameter. That is, the computer has images of the nearly same size for different pellets.

3. Inspection of Geometrical Form

The computer image of a pellet consists of three regions: (1) background, (2) a dark ring (the side of a pellet), and (3) a bright center circle (a contact surface). Since the averaged gray levels in these three regions are clearly different, we adopt the simple thresholding technique to extract each of three regions.

Two border lines of the neighboring regions are two circles whose center are located nearly at the same place. Inspection of geometrical form is entirely based on thus extracted two digitized circles.

3.1 Detection of Fins and Cracks

Since a fin or a crack is defined as a deform on a short arc of a circle, we decide to measure a length of an arc on a predetermined interval. Write the coordinate of a point on a circle of a digital image successively as (x_i, y_i) $(i=1,2,\ldots,n)$. As the center of the digitized circle is estimated by the average of these points, the coordinate of the center $(\bar{x}, \bar{y})$ is calculated by

$$x=\frac{1}{n}\sum_{i=1}^{n} x_i, \quad y=\frac{1}{n}\sum_{i=1}^{n} y_i \quad (1)$$

We place a cartesian coordinate on the circle, where $(\bar{x}, \bar{y})$ is on the origin of the coordinate.

Draw a half line originated from the origin whose angle is θ from the

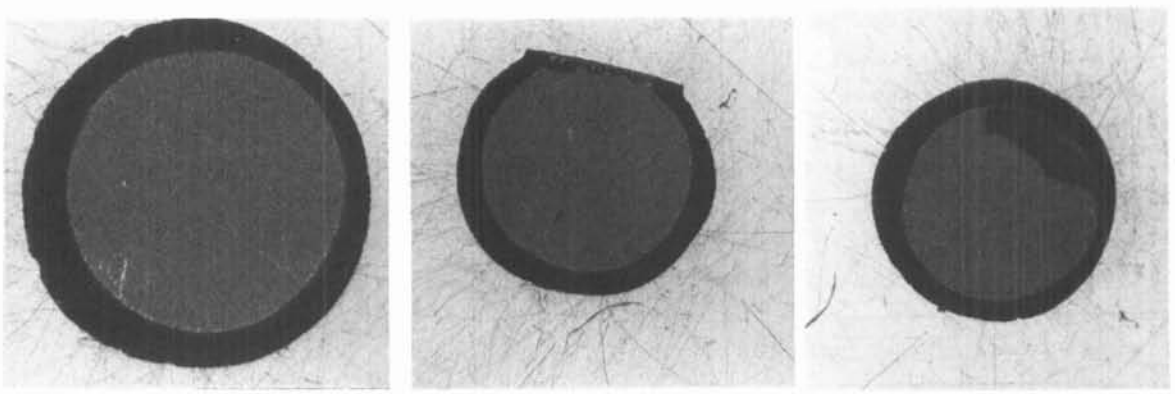

(a) (b) (c)

Fig.3 Three typical photographs:(a) normal,(b) deformed,and (c) stained pellet.

horizontal axis, and also two more lines before and after the first line, whose relative distance are $+\vartheta$ and $-\vartheta$, respectively. Thus drawn two lines($\theta+\vartheta$ and $\theta-\vartheta$) defines an arc on a circle. In our experiments ϑ is fixed as 10 degree, so we drop the variable ϑ in the following expressions. Using the digital picture processing technique we calculate the length of the given arc. Write the calculated length as $L(\theta)$.

So as to make $L(\theta)$ dimensionless, we have to computer a representative length of a circle, which, we decide, is the minimum of digital radii. A radius of a point on a digital circle is computed by

$$R(x_i,y_i)=\sqrt{(x_i-\bar{x})^2+(y_i-\bar{y})^2} \quad . (2)$$

Then, the shortest of them is expressed by

$$R_{min}=\min_{i} R(x_i,y_i). \quad (3)$$

Dividing $L(\theta)$ by R_{min}, we have

$$\ell(\theta)=\frac{L(\theta)}{R_{min}} \quad (4)$$

which is non-dimensional. By our experiences the adoption of R_{min} amplifies a faulted arc. Two examples of the measured results for a normal and a defected pellet are drawn in Fig. 4, where $\ell(\theta)$ of a normal pellet is indicated by a solid line, and a defected pellet by a dotted line. Clearly the variation of the dotted line is larger than the solid line.

Since good pellets themselves have their own distribution, we have to compute the statistics of the normal set of pellets. Write the number of the member of the normal set as K. After measurements we have $\ell_k(\theta)$ $(k=1,2,\ldots K)$. An average on the point is calculated by

$$\bar{\ell}(\theta)=\frac{1}{K}\sum_{k=1}^{K}\ell_k(\theta), \quad (5)$$

and the standard deviation is

$$\sigma(\theta)=\sqrt{\frac{1}{K}\sum_{k=1}^{K}(\ell_k(\theta)-\bar{\ell}(\theta))^2} \quad . (6)$$

The actual results are shown in Fig. 5, where $\bar{\ell}(\theta)$ is shown in a dotted line, and two solid lines are

$$\left.\begin{aligned}\ell^*(\theta)&=\bar{\ell}(\theta)+3\sigma(\theta),\\ \ell_*(\theta)&=\bar{\ell}(\theta)-3\sigma(\theta)\end{aligned}\right\} \quad (7)$$

respectively. $\ell^*(\theta)$ and $\ell_*(\theta)$ is two representative lines which limit the distribution of the acceptable samples.

At this moment, assume we made a measurement on an unknown pellet. Write the result as $\ell(\theta)$. Then, we compute the difference of $\ell(\theta)$ from $\ell^*(\theta)$ or $\ell_*(\theta)$. That is, we define

$$\left.\begin{aligned}&\text{if } \ell(\theta)>\ell^*(\theta) \quad \text{then } \delta_\ell(\theta)=\ell-\ell^*\\ &\text{if } \ell(\theta)<\ell_*(\theta) \quad \text{then } \delta_\ell(\theta)=\ell_*-\ell\\ &\text{if } \ell_*(\theta)\leqq\ell(\theta)\leqq\ell^*(\theta) \quad \text{then } \delta_\ell(\theta)=0\end{aligned}\right\} \quad (8)$$

and calculates its mean square error as

$$E_\ell=\sqrt{\frac{1}{m}\Sigma\delta_\ell^2} \quad . (9)$$

We have in advance decided a thresholding value T_ℓ from the experiments, and concerning the measured E_ℓ

$$\left.\begin{aligned}&\text{if } E_\ell>T_\ell,\\ &\quad\text{then the pellet is rejected,}\\ &\text{if } E_\ell\leqq T_\ell,\\ &\quad\text{then the pellet is accepted}\end{aligned}\right\} \quad (10)$$

is the final decision.

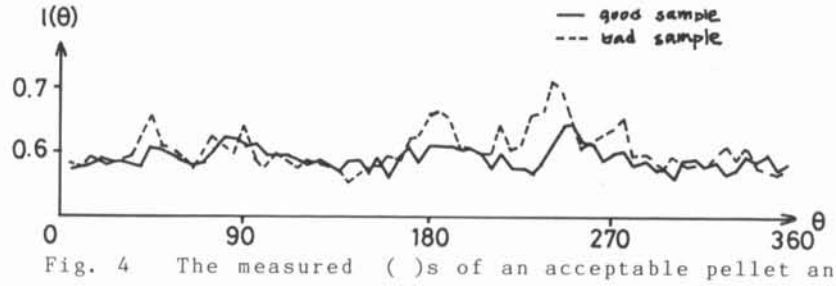

Fig. 4 The measured ( )s of an acceptable pellet and a defect pellet.

4. Results

On a set of 1000 good samples, we have carried out measurements and computations. All the necessary statistics and thresholding values are determined. Then, other 800 samples are brought into our laboratory. Our experimental results are listed in Table 1. In a summary about 750 samples from 800, the computer made the same decision as human inspectors, while 50 decisions is split between our computer and the human judgments.

We investigated the 50 cases of the split decision. 24 out of 50 are recognized as the error of human side, and 26 are of the computer. Thus, the final correct decision rate of the computer raises to 96.7 %.

We think that concerning at least the inspection problem of diode pellets, the computer can be substituted for human inspecting workers. We believe that the computer power helps to liberate human resources to other more creative works.

5. References

[1] G. J. Vanderbrug and R. N. Nagel, Image Pattern Recognition in Industrial Inspection, NBSIR 79-1764, 1974.

[2] G. B. Poter and J. L. Mundy, Visual Inspection Systems Design, IEEE Computer, May 1980, pp. 40-48.

[3] J. V. Daele, A. Oosterlinck, and H. Van den Berghe, Automatic Visual Inspection of Reed Switches, Optical Engineering, Vol. 19 No. 2, 1980, pp. 240-244.

[4] J. F. Jarvis, A Method for Automating the Visual Inspection of Printed Wiring Boards, IEEE Trans. on Pattern Analysis and Machine Intelligence, Vol. PAMI-2 No. 1, 1980.

[5] E. Fletcher, MIDAS-High Speed Automatic Surface Inspection of Steel Billets, IPC Business Press, Vol. 12 No. 4, 1979, pp. 163-166.

[6] Y. Okawa, Automatic Inspection of the Surface Defects of Cast Metals, Computer Vision, Graphics and Image Processing, Vol. 25, 1984, pp. 82-112.

Fig. 5 The upper and lower limits of the acceptable pellets.

	Good samples	bad samples	Total
φ 1.85 pellets	$\frac{186}{200} = 93.0\%$	$\frac{189}{200} = 94.5\%$	$\frac{375}{400} = 93.8\%$
φ 2.8 pellets	$\frac{190}{200} = 95.0\%$	$\frac{185}{200} = 92.5\%$	$\frac{375}{400} = 93.8\%$
Total	$\frac{376}{400} = 94.0\%$	$\frac{374}{400} = 93.5\%$	$\frac{750}{800} = 93.8\%$

Table 1 The experimental results.